Magnetic resonance microscopy at 17.6-Tesla on chicken embryos in vitro

Hogers, B.; Gross, D.; Lehmann, V.; Groot, H.J.M. de; Roos, A. de; Gittenberger-De Groot, A.C.; Poelmann, R.E.

Technical Note

Magnetic Resonance Microscopy at 17.6-Tesla on Chicken Embryos In Vitro

Bianca Hogers, PhD,[1] Dieter Gross, PhD,[2] Volker Lehmann, PhD,[2] Huub J.M. de Groot, PhD,[3] Albert de Roos, MD,[4] Adriana C. Gittenberger-de Groot, MD,[1] and Robert E. Poelmann, PhD[1]*

The non-destructive nature and the rapid acquisition of a three-dimensional image makes magnetic resonance microscopy (MRM) very attractive and suitable for functional imaging investigations. We explored the use of an ultra high magnetic field for MRM to increase image quality per image acquisition time. Improved image quality was characterized by a better signal-to-noise ratio (SNR), better image contrast, and higher resolution compared to images obtained at lower magnetic field strengths. Fixed chicken embryos at several stages of development were imaged at 7.0-T (300 MHz) and at 17.6-T (750 MHz). Maximum intensity projection resulted in three-dimensional vascular images with ample detail of the embryonic vasculature. We showed that at 750 MHz frequency, an image with approximately three times better SNR can be obtained by T_1-weighting using a standard gadolinium contrast agent, compared to the same measurement at 300 MHz. The image contrast improved by around 20 percent and the contrast-to-noise ratio improved by almost a factor of 3.5. Smaller blood vessels of the vascular system were identified at the high field, which indicates a better image resolution. Thus, ultra high field is beneficial for MRM and opens new areas for functional imaging research, in particular when SNR, resolution, and contrast are limited by acquisition time. J. Magn. Reson. Imaging 2001;14:83–86.

Index terms: heart development; magnetic resonance imaging; vascular development; ultra high field; contrast

ABNORMALITIES OF THE HEART and great arteries of experimental animals, such as transgenic mice, often cause intrauterine death. This raises a need for rapid, sensitive, and non-invasive imaging methods to complement existing methods for diagnosing problems in transgenic mouse embryos and newborn pups in preclinical studies. Traditional methods of analyzing congenital anomalies involve either sectioning and stacking slices for light microscopy or preparing vascular casts for scanning electron microscopy. Acquiring useful spatial images with these methods is time-consuming, and even with the use of advanced image processing software (1,2), there is always the risk of distortion, artifacts, and degradation of spatial resolution.

A relatively new approach is magnetic resonance microscopy (MRM), an imaging technique that explores the nuclear magnetic characteristics of the abundant protons in the tissues (3,4). With modern state-of-the-art equipment, resolution of 12 μm can be obtained (5). This is adequate for diagnostic purposes. The value of three-dimensional images of fixed transgenic mouse embryos was demonstrated by the diagnosis of the conotruncal heart malformations in Connexin 43 knockout and transgenic mice (4). The ultimate use for MRM is the possiblity of monitoring living embryos during development. However, acquisition time is often the major limitation when using MRM for in vivo studies. Imaging at ultra high fields is thus quite promising since the signal-to-noise ratio (SNR) increases linearly with the field strength (6). The relationship between SNR and acquisition time is $s/n \propto \sqrt{t}$, where s is the signal, n is the noise, and t is the acquisition time (5). An increase in the field strength increases the SNR of a given voxel volume (resolution) with a constant factor, so that the acquisition time is decreased with the square of that factor, yielding an image with the same SNR and resolution. Susceptibility differences caused by interior inhomogeneities of the objects, however, may reduce the actual spatial resolution at very high magnetic fields. These inhomogeneity effects are proportional to the field strength, but they can be reduced by applying stronger magnetic field gradients during the imaging experiment (7).

Following improvements in superconducting wire technology, advancements in nuclear magnetic resonance magnet design, and implementation of a supercooled cryostat concept, a wide bore 750 MHz, 17.6-T magnet has been constructed. In this study, we ex-

[1]Department of Anatomy, Leiden University Medical Center, Leiden, The Netherlands.

[2]Bruker Analytic GmbH, Rheinstetten, Germany.

[3]Leiden Institute of Chemistry, Leiden University, Leiden, The Netherlands.

[4]Department of Radiology, Leiden University Medical Center, Leiden, The Netherlands.

Contract grant sponsor: Commission of the European Communities; Contract grant number: BIO4-CT97-2101; Contract grant sponsor: Leiden University, Grant-in-aid.

Presented at the 7th Annual Meeting of ISMRM, Philadelphia, 1999.

*Address reprint requests to: R.E.P., Department of Anatomy, Leiden University Medical Center, Wassenaarseweg 62, 2333 AL Leiden, The Netherlands. E-mail: R.E.Poelmann@LUMC.nl

Received August 31, 2000; Accepted December 27, 2000.

plored the capacities of this new instrument for MRM imaging purposes. Recent studies on embryonic development have been restricted to low, 4–T fields (8) and moderately high fields, up to 9.4-T (5,9). The results of this study can be used to estimate the experimental parameters for future in vivo studies.

METHODS

Embryo Collection

Fertilized White Leghorn eggs (Gallus domesticus) were incubated at 37°C and 60%–70% relative humidity for 3–5 days, until stages 15, 24, or 29, according to the age determination criteria of Hamburger and Hamilton (10).

For fixation and mounting of the embryos, the technique of Smith and coworkers (3) was used. Briefly, warm (37°C) phosphate-buffered saline was perfused into the omphalomesenteric vein with a glass needle, followed by a fixative perfusion (2% glutaraldehyde/1% formaldehyde in phosphate buffer). Subsequently, a gadolinium contrast agent [bovine serum albumin-diethylene triamine pentaacetic acetate-gadolinium chloride (1mM) mixed with 5% gelatin] was injected. Embryos were immersion-fixed at 4°C to solidify the gelatin, and transferred to plastic containers filled with proton-free perfluoro-polyether Fomblin (Ausimont Inc., Bollate, Italy). The size of the containers was chosen to be as small as possible to immobilize the embryo without disturbing its natural conformation.

Magnetic Resonance Microscopy

Embryos were imaged using either a 300 MHz (7.0-T), 150-mm vertical bore magnet (AVANCE console) or a 750 MHz (17.6-T), 89-mm vertical bore magnet (DSX-750 console, both from Bruker Analytic, Rheinstetten, Germany). The novel 750 MHz spectrometer was equipped with a 89-mm bore shim unit with an inner diameter of 72 mm. Both systems were connected to microimaging accessories, a gradient system of 100 G/cm, and the Micro2.5 probe with exchangeable rf-coils. We used a 4-mm solenoid coil for the stage 15 embryo, a 10-mm birdcage coil for the stage 24 embryo, and a 15-mm birdcage coil for the stage 29 embryo. The same coils were used in both magnets.

Each session began with a multislice orthogonal gradient-echo sequence for position determination and selection of the desired region for subsequent experiments.

We used three-dimensional spin-echo for the imaging data sets. For the stage 15 embryo, the matrix size was $256 \times 128 \times 128$, the echotime (TE) was 4 msec, the repetition time (TR) was 100 msec, and a signal average of 2 was used for each phase encoding step. For the other embryos (stage 24 and 29), the matrix size was $256 \times 256 \times 256$, the TE was 6 msec, the TR was 200 msec, with four averages. The field of view (FOV) was adjusted to match the size of the embryo and the total experiment time (T) was adapted accordingly. For stage 15, the FOV was $8 \times 4 \times 4$ mm and T was 53 minutes; for stage 24, the FOV was $10 \times 10 \times 10$ mm and T was 14 hours and 33 minutes; and for stage 29, the FOV was $14 \times 14 \times 14$ mm and T was 14 hours and 33 minutes (300 MHz) or 14 hours and 46 minutes (750 MHz).

Data acquisition and processing were performed with ParaVision (Bruker, Rheinstetten, Germany) running on a Silicon Graphics O2 workstation with the Irix 6.5.3 operating system.

RESULTS

The images obtained at 300MHz from the embryos at three intermediate states of development are shown in Figure 1. The increasing complexity of the vascular system was clearly visible. An intravascular contrast agent was used for image enhancement, and maximum intensity projections were obtained from the data sets. The oldest embryo (stage 29, Fig. 1c) was also imaged in the 750 MHz magnet (Fig. 1d). To collect the high field image, we used exactly the same parameter settings for TR (200 msec) and TE (6 msec) to study the improvement of image quality, rather than shortening the total scan time. SNR was defined as (mean signal intensity)/(standard deviation of the noise), and was determined at various positions in the three-dimensional images acquired at 300 MHz and at 750 MHz. The values are shown in Table 1. The higher magnetic field improved the SNR by a factor 2.96 in tissues (no contrast agent) and by a factor of 3.4 in the blood vessels (with contrast agent). The difference between these SNR improvement factors may be due to differences in the saturation of the magnetization and in the T2 relaxation times in the tissues with and without contrast agent in the two experiments. Further experiments are needed to determine the T1 and T2 relaxation times of the tissues (without contrast agent) and blood vessels (with contrast agent) at the two different field strengths. The contrast between the blood vessels and the other tissues was determined as C = (mean intensity difference between tissues with and without contrast agent)/(mean intensity of tissue without contrast agent) (11) at various positions in the three-dimensional images obtained at 300 MHz and 750 MHz, respectively. The values are shown in Table 1. The gain in contrast ($C_{750\ MHz}/C_{300\ MHz}$) was approximately 20 percent. Faster repetition times might increase the contrast but with the risk of reducing the overall SNR.

The image acquired at 750MHz (Fig. 1d) showed essentially the same vascular pattern as that acquired at 300 MHz (Fig. 1c) but with a better contrast-to-noise ratio (CNR). The CNR was the difference between the SNR values from tissue with and without contrast agent (11) at various positions in the three-dimensional images acquired at 300 MHz and 750 MHz, respectively (see Table 1). A gain of a factor of 3.5 was observed in the images at 750 MHz. Small vessels that were beyond detection in the 300 MHz image, especially in the brain and eyes, could be visualized with the 750 MHz MRM. There was also more detail visible within the heart. In particular, details of the atria, ventricles, and outflow tract, which are hardly visible in the 300 MHz image, form clearly separate structures in the ultra high field image of Figure 1d. This indicates that susceptibility effects do not cause a loss of structural information in fixed chicken embryo samples, even at the very high

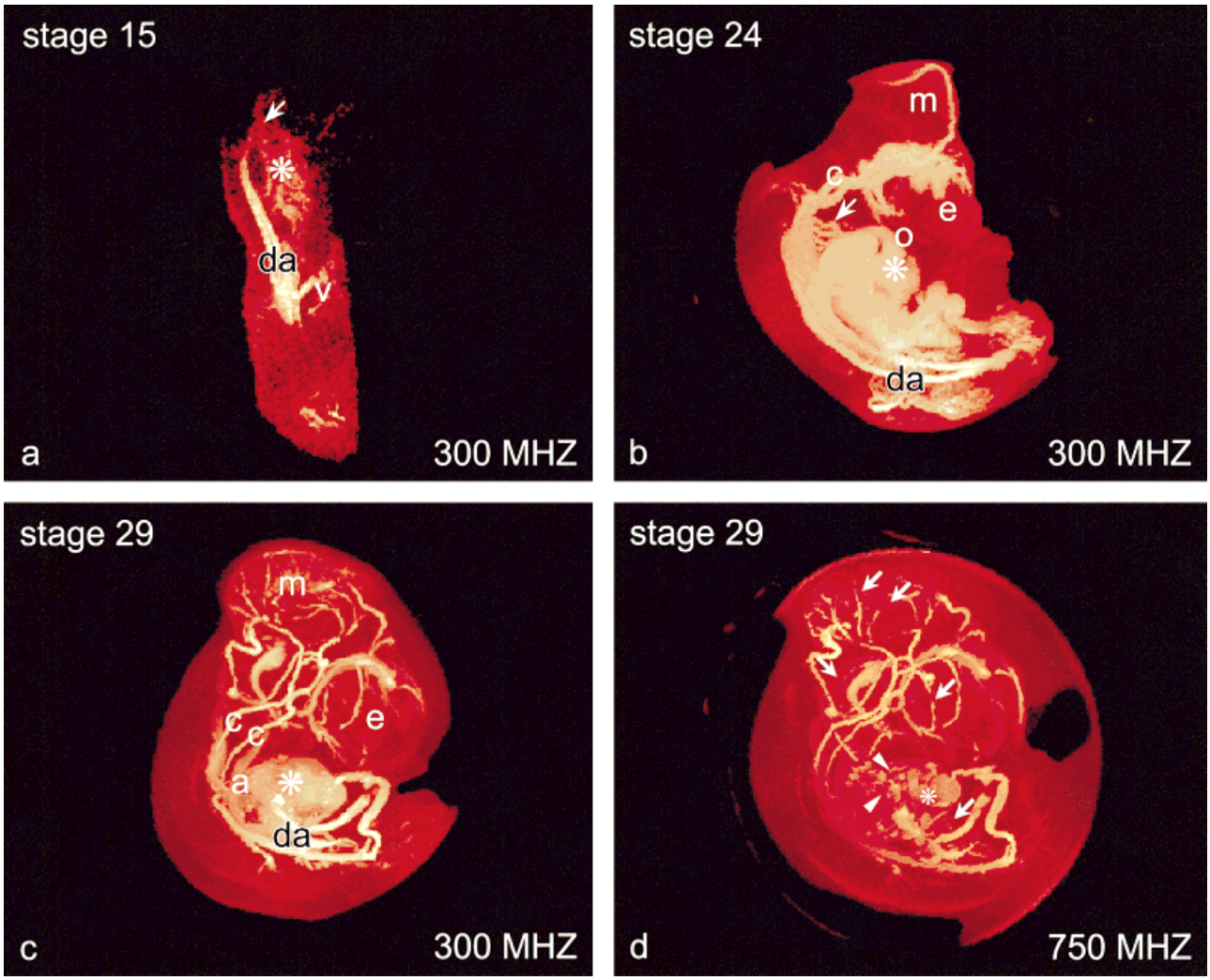

Figure 1. Maximum intensity projections of intravascular gadolinium contrast-enhanced chicken embryos obtained with a three-dimensional spin-echo imaging method. (**a**) Stage 15 embryo: The looped heart (asterisk) and pharyngeal arch arteries (arrow) are visible. FOV = 8 × 4 × 4 mm, resolution (R) = 31 × 31 × 31 μm. (**b**) Stage 24 embryo: The heart (asterisk), the pharyngeal arch arteries (arrow), the cranial vasculature, the dorsal aortae and branches and the venous system are shown. FOV = 10 × 10 × 10 mm, R = 39 × 39 × 39 μm. (**c**) Stage 29 embryo: The brain and eye vasculature is very prominent. The pharyngeal arch artery system has evolved in the final pattern with one right-sided aortic arch, which is characteristic for birds. The venous system is present with the main branches. FOV= 14 × 14 × 14 mm, R = 55 × 55 × 55 μm. (**d**) The same embryo imaged at 17.6-T, using the same instrument settings as in (c), yielded better contrast. This is demonstrated by the appearance of traces of smaller vessels (arrows) that were not observed in the 300 MHz image. There is also more detail within the heart (asterisk), like the atria (arrow head), ventricles, and outflow tract (arrow head) that are hardly separate structures in the 300 MHz image. FOV = 14 × 14 × 14 mm, R = 55 × 55 × 55 μm. a = anterior cardinal vein, c = carotid arteries, da = dorsal aortae, e = eye, m = midbrain, and v = vitelline artery.

field of 17.6-T. The influence of the better SNR and CNR resulted in more structural information.

DISCUSSION

To our knowledge, this is the first report of embryonic imaging at 17.6-T. The results show considerable improvement relative to current practice (3). The image quality for the smaller vessels improved considerably, and the CNR within structures was better than in the comparable images obtained at 300 MHz. The improved performance at 750 MHz was mainly attributed to the improved sensitivity. Since the experimental parameters were held constant while the SNR improved with

Table 1
Image Quality Improvement From 300 to 750 MHz

Variables[a]	300 MHz	750 MHz	Gain
$SNR_{Tissue\ without\ Gd}$	27	80	2.96
$SNR_{Tissue\ with\ Gd}$	119	405	3.4
Contrast	3.4	4.07	1.20
CNR	92	325	3.5

[a]SNR = signal-to-noise ratio, and was defined as mean signal/standard deviation of noise; Contrast is defined as $(Intensity_{position\ A} - Intensity_{position\ B})/Intensity_{position\ B}$; CNR = contrast-to-noise ratio, and was defined as $SNR_{with\ Gd} - SNR_{without\ Gd}$; Gd = the intravascular contrast agent gadolinium ('Bovine Serum Albumine – Diethylene Triamine Pentaacetic Acetate – Gadolinium chloride' (1 mM) mixed with 5% gelatin).

increasing field strength, we measured an increase in SNR by a factor of approximately 3.4 at 17.6-T compared to 7-T. We have not performed an in-depth investigation of the field dependence of the relaxation parameters. However, the trend for the relaxation times towards higher fields is an increase of T1 and a decrease of T2. This has been observed in fields up to 500 and 600 MHz (unpublished results). Saturation effects and T2 relaxation will reduce the SNR if the repetition and echo times are not optimized in the ultra high field experiments. Since our experiments were performed with exactly the same repetition and echo times at 300 MHz and 750 MHz, further increases in the SNR can be expected upon adjustment of these parameters. Further experiments are planned to verify the exact T1 and T2 relaxation times of the tissues with and without contrast agent.

Imaging with the 750 MHz magnet is promising for future embryology studies since younger embryos with even smaller blood vessel diameters can be studied in detail. There is an improvement of vessel size recognition in the 750 MHz instrumentation; we were even able to visualize the very small diameter vessels like the dorsal intersegmental arteries, although not in every stage. We attribute this to the high viscosity of the contrast agent. It appears necessary to optimize the contrast agent properties in order to find a balance between maximal perfusion of the smallest embryonic vessels (low viscosity) and maximum gadolinium fixation inside the vessels, which requires a more viscous agent. For the images shown in Figure 1, a 5% gelatin concentration was used, which is half of the gelatin concentration used in other studies (3).

Although studying vascular corrosion casts with e.g., scanning electron microscopy (12–14) yields a resolution that can never be obtained by MRM, additional histology or immunohistochemistry cannot be performed, as all tissues are digested in the process. The value of MRM thus lies in the fact that, since it is non-invasive and non-deleterious, it can complement other analytical tools. After complete MRM examination, the sample can be processed for other studies. This is an important advantage when the object is a very rare specimen, like a transgenic animal model.

CONCLUSIONS

Herein we demonstrated that the imaging of embryos with good contrast and resolution was feasible at the current level of ultra high magnetic field technology. Improvements in the resolution can be expected in the near future, with better optimization of the high field imaging parameters and further technological improvements. The development of high field imaging of living embryos in a reasonable period of time opens the way for longitudinal studies of the development of the cardiovascular system and of the ontogeny of cardiovascular anomalies in individual embryos.

ACKNOWLEDGMENTS

The authors thank B. Smith for introducing us to the world of magnetic resonance microscopy and C. Erkelens, P. Kunz and J. Doornbos for their technical advice and critical reading of the manuscript.

REFERENCES

1. Poelmann RE, Verbout AJ. Computer-aided three-dimensional graphic reconstructions in a radiological and anatomical setting. Acta Anat 1987;130:132–136.
2. Streicher J, Weninger WJ, Muller GB. External markers based automatic congruencing: a new method of 3D-reconstruction from serial sections. Anat Rec 1997;248:583–602.
3. Smith BR, Johnson GA, Groman EV, Linney E. Magnetic resonance microscopy of mouse embryos. Proc Natl Acad Sci U S A 1994;91:3530–3533.
4. Huang GY, Wessels A, Smith BR, Linask KK, Ewart JL, Lo CW. Alteration in connexin 43 gap junction gene dosage impairs conotruncal heart development. Dev Biol 1998;198:32–44.
5. Smith BR, Linney E, Huff DS, Johnson GA. Magnetic resonance microscopy of embryos. Comp Med Imag Graph 1996;20:483–490.
6. Vlaardingerbroek MT, DeBoer JA. Magnetic resonance imaging. Berlin, Heidelberg, New York: Springer Verlag; 1996.
7. Callaghan PT. In: Principles of Nuclear Magnetic Resonance Microscopy. Oxford: Clarendon Press; 1991.
8. Hoydu AK, Kitano Y, Kriss A, Hensley H, Bergey P, Flake A, Hubbard A, Leigh JS. In vivo, in utero magnetic resonance imaging: application in a rat model of diaphragmatic hernia. Magn Reson Med 2000;44:331–335.
9. Hogers B, Gross D, Lehmann V, Zick K, DeGroot HJM, Gittenberger-De Groot AC, Poelmann RE. Magnetic resonance microscopy of mouse embryos in utero. Anat Rec 2000;260:373–378.
10. Hamburger V, Hamilton HL. A series of normal stages in the development of the chick embryo. J Morphol 1951;88:49–92.
11. Kanal E, Wehrli FW. Signal-to-noise ratio, resolution and contrast. In: Wehrli FW, Shaw D, and Kneeland JB, editors. Biomedical magnetic resonance imaging. Principles, methodology, and applications. Weinheim, New York, Basel, Cambridge: VCH; 1988;47–114.
12. DeRuiter MC, Hogers B, Poelmann RE, VanIperen L, Gittenberger-de Groot AC. The development of the vascular system in quail embryos: a combination of microvascular corrosion casts and immunohistochemical identification. Scanning Microsc 1991;5:1081–1090.
13. Aharinejad S, FFranz P, Lametschwandtner A, Firbas W. Esophageal vasculature in the guinea pig: a scanning electron microscope study of vascular corrosion casts. Scanning Microsc 1989;3:567–574.
14. Ditrich H, Splechtna H. The opisthonephric blood vascular system of the chicken embryo as studied by scanning electron microscopy of microvascular corrosion casts and critical point dried preparations. Scanning Microsc 1989;3:559–565.